Generalized ℓ_2-ℓ_p Minimization Based DOA Estimation for Sources with Known Waveforms in Impulsive Noise

Yang-Yang Dong[a,*], Chun-Xi Dong[a], Wei Liu[b], Jingjing Cai[a]

[a]*School of Electronic Engineering, Xidian University, Xi'an 710071, China*
[b]*Department of Electronic and Electrical Engineering, University of Sheffield, S1 4ET, U.K.*

Abstract

The direction of arrival (DOA) estimation problem for sources with known waveforms in the presence of impulsive noise is studied. To solve the problem, the impulsive noise is decomposed into Gaussian and sparse parts, and a generalized ℓ_2-ℓ_p minimization based cost function is developed by setting generalized Gaussian distribution (GGD) as the prior distribution of sparse part. Then, to solve this nonconvex problem, the generalized ℓ_2-ℓ_p problem is decoupled into multiple independent and dimension reduced simple ℓ_2-ℓ_p optimization problems with respect to the sparse part, and solved under the accelerated proximal gradient framework. Finally, DOAs and complex amplitudes are estimated from the cleaned data. As demonstrated by simulation results, the proposed method has a better performance than existing ones in the presence of Gaussian mixture model (GMM) and GGD noise, while it is comparable for symmetric α stable (SαS) noise.

Keywords: Direction of arrival estimation, known waveform, impulsive noise, nonconvex optimization.

---
*Corresponding author
 Email address: dongyangyang2104@126.com (Yang-Yang Dong)

1. Introduction

Direction of arrival (DOA) estimation has a wide range of applications in wireless communications, radar, and sonar, etc [1]. There are many conventional methods developed, such as maximum likelihood (ML) [2], subspace fitting (SF) [3], multiple signal classification (MUSIC) [4], and estimation of signal parameters via rotational invariance technique (ESPRIT) [5].

To further improve their performance, many researchers have utilized the known signal waveform for angle estimation and better performance has been achieved [6–18]. According to the required waveform information, there are two main types: one is for the ideal waveform scenario, such as decoupled maximum likelihood (DEML) [7], subarray beamforming (SB) [8], linear regression (LR) [9], and structured least squares (SLS) [11]; the other one is for waveforms disturbed by some unknown factors, such as Doppler shift and time delay [16–18]. Importantly, all of these methods have assumed that the noise follows a Gaussian distribution.

However, it has been witnessed that the non-Gaussian and impulsive noise model may fit the real-world scenario better for many applications [19–25]. To model the impulsive property, many typical probability density functions (PDFs) have been developed, including the Gaussian mixture model (GMM) [19], the generalized Gaussian distribution (GGD) [20], the symmetric α-stable (SαS) distribution [21], spherically invariant random process (SIRP) [24], and complex elliptically symmetric (CES) distributions [25], where the former three models are considered in this paper. With the aid of waveform information, an ln-ℓ_p^ε method was proposed to estimate DOAs in the presence

2

of SαS noise [26]. However, the method can only suppress the outliers, and cannot utilize the potential property of impulsive noise to improve estimation performance further.

To estimate the DOAs for sources with known waveforms in the presence of impulsive noise better, inspired by the work in [27, 28], we divide the impulsive noise into two components: the Gaussian part and the remaining sparse part. Following the principle of maximum a posteriori (MAP), a generalized ℓ_2-ℓ_p nonconvex minimization cost function is constructed by considering GGD as the prior distribution of sparse noise. Then, using orthogonal projection and the component additivity of ℓ_p norm, we decouple the generalized ℓ_2-ℓ_p problem into multiple independent and dimension reduced conventional ℓ_2-ℓ_p optimization problems with respect to the sparse noise, and obtain the estimate of sparse part via the accelerated proximal gradient (APG) framework. Finally, with the aid of estimation of the sparse noise part, the original noise is reduced to Gaussian and the DOAs and complex amplitudes are then calculated in the usual way for Gaussian noise. Simulation results show that the proposed method has better performance than the state of the art under GMM and GGD noise, and comparable to the existing methods under SαS noise. Moreover, the performance of the proposed method can approach the Cramer-Rao bound (CRB) in the presence of GMM noise at high SNR with a large number of snapshots. Further, there is no specific restrictions to the impulsive noise model for the proposed method, and other impulsive or heavy-tailed noise models, such as SIRP and CES noises, could also be used.

Notations: matrices and vectors are denoted by boldfaced capital letters

and lower-case letters, respectively. $(\cdot)^T$ $(\cdot)^H$, $(\cdot)^{-1}$, $(\cdot)^{\dagger}$, $\otimes$, and $\circ$ stand for transpose, conjugate transpose, inverse, Moore-Penrose inverse, Kronecker product, and Hadamard product, respectively. $\text{vec}\{\cdot\}$, $\text{diag}\{\cdot\}$, $\|\cdot\|_p$, and $\|\cdot\|_F$ denote the vectorization, diagonalization, ℓ_p norm, Frobenius norm, respectively. $\text{angle}\{\cdot\}$, $\text{Re}\{\cdot\}$, and $\text{Im}\{\cdot\}$ represents the phase, real and imaginary parts of a complex number, respectively.

2. Data Model

Consider a uniform linear array (ULA) of M sensors with inter-sensor spacing d. There are Q narrowband far-field uncorrelated sources with known waveforms $\{s_q(n)\}_{q=1}^Q$ ($n = 0, \cdots, N-1$, with N being the number of snapshots) of wavelength λ impinging from unknown directions $\{\theta_q\}_{q=1}^Q$ with unknown complex amplitudes $\{g_q\}_{q=1}^Q$. The received data matrix of N snapshots can be expressed as

$$\mathbf{X} = \mathbf{A}(\boldsymbol{\theta})\mathbf{G}(\mathbf{g})\mathbf{S} + \mathbf{W} = \mathbf{B}(\boldsymbol{\theta}, \mathbf{g})\mathbf{S} + \mathbf{W} \tag{1}$$

where

$$\mathbf{X} = [\mathbf{x}(0), \mathbf{x}(1), \cdots, \mathbf{x}(N-1)],$$

$$\mathbf{x}(n) = [x_1(n), x_2(n), \cdots, x_M(n)]^T,$$

$$\mathbf{A}(\boldsymbol{\theta}) = [\mathbf{a}(\theta_1), \mathbf{a}(\theta_2), \cdots, \mathbf{a}(\theta_Q)],$$

$$\mathbf{a}(\theta_q) = [1, e^{-j2\pi d \sin\theta_q/\lambda}, \cdots, e^{-j2\pi(M-1)d\sin\theta_q/\lambda}]^T,$$

$$\boldsymbol{\theta} = [\theta_1, \theta_2, \cdots, \theta_Q]^T,$$

$$\mathbf{G}(\mathbf{g}) = \text{diag}\{g_1, g_2, \cdots, g_Q\},$$

$$\mathbf{g} = [g_1, g_2, \cdots, g_Q]^T,$$

$$\mathbf{S} = [\mathbf{s}(0), \mathbf{s}(1), \cdots, \mathbf{s}(N-1)],$$

$$\mathbf{s}(n) = [s_1(n), s_2(n), \cdots, s_Q(n)]^T,$$

$$\mathbf{W} = [\mathbf{w}(0), \mathbf{w}(1), \cdots, \mathbf{w}(N-1)],$$

$$\mathbf{w}(n) = [w_1(n), w_2(n), \cdots, w_M(n)]^T.$$

$\mathbf{A}(\boldsymbol{\theta})$, $\mathbf{a}(\theta_q)$, and $\mathbf{g}$ are often called as the array manifold matrix, steering vector, and complex amplitude vector.

Similar to [20, 26], we assume the additive noise $\mathbf{W}$ is statistically uncorrelated with the signal $\mathbf{S}$, and follows one of the three mentioned impulsive noise distributions. Besides, without causing confusion, $\mathbf{B}(\boldsymbol{\theta}, \mathbf{g})$ is simplified to $\mathbf{B}$ in the following derivations.

3. Proposed Method

3.1. Cost function construction based on generalized ℓ_2-ℓ_p optimization

According to [27, 28], the data model in (1) can be rewritten as

$$\mathbf{X} = \mathbf{BS} + \mathbf{U} + \mathbf{V} \tag{2}$$

where $\mathbf{U}$ and $\mathbf{V}$ represent the Gaussian part of noise, and the remaining sparse outlier part, respectively. [1] Moreover, $\mathbf{V}$ is of row sparsity.

Now vectorize (2) as follows

$$\mathbf{x} = (\mathbf{S}^T \otimes \mathbf{I}_M)\mathbf{b} + \mathbf{u} + \mathbf{v} \tag{3}$$

where $\mathbf{x} = \text{vec}(\mathbf{X})$, $\mathbf{b} = \text{vec}(\mathbf{B})$, $\mathbf{u} = \text{vec}(\mathbf{U})$, $\mathbf{v} = \text{vec}(\mathbf{V})$. $\mathbf{I}_M$ is the identity matrix of size M.

---

[1] There is no specific restrictions to noise model as long as the noise can be decomposed into Gaussian plus sparse outliers with some acceptable approximation errors.

Since $\mathbf{U}$ is Gaussian, we assume $\mathbf{u} \sim CN(0, \sigma_u^2 \mathbf{I}_{MN})$, and its PDF can be expressed as

$$p(\mathbf{u}) = \frac{1}{\pi^{MN} \sigma_u^{2MN}} \exp \left\{ -\frac{1}{\sigma_u^2} \mathbf{u}^H \mathbf{u} \right\} \tag{4}$$

where σ_u^2 denotes the variance of Gaussian noise part.

Then, the conditional PDF of $p(\mathbf{x}|\mathbf{v}; \mathbf{b})$ also follows the multi-variate complex Gaussian distribution, i.e.,

$$p(\mathbf{x}|\mathbf{v}; \mathbf{b}) = \frac{1}{\pi^{MN} \sigma_u^{2MN}} \exp \left\{ -\frac{1}{\sigma_u^2} ||\mathbf{x} - (\mathbf{S}^T \otimes \mathbf{I}_M)\mathbf{b} - \mathbf{v}||_2^2 \right\} \tag{5}$$

According to the MAP principle, an assumption about the a priori PDF of sparse noise $\mathbf{v}$ is needed. As discussed in [29], the i.i.d. zero-mean Laplacian distribution prior is of particular interest for sparse signals. However, to be more general, the i.i.d. zero-mean complex GGD is used as the prior

$$p(\mathbf{v}) = \left[\frac{\beta \Gamma(4/\beta)}{2\pi \sigma_v^2 \Gamma^2(2/\beta)} \right]^{MN} \exp \left\{ -\frac{1}{\sigma_v^\beta} \left[\frac{\Gamma(4/\beta)}{\Gamma(2/\beta)} \right]^{\beta/2} ||\mathbf{v}||_\beta^\beta \right\} \tag{6}$$

where β, σ_v^2, and $\Gamma(\cdot)$ denote the shape parameter, variance and Gamma function. For $\beta = 2$, GGD represents the Gaussian distribution; when $\beta > 2$, GGD models short-tailed noise, while for $0 < \beta < 2$, it yields the heavy-tailed one, i.e., impulsive noise. For $\beta = 1$, GGD becomes the Laplacian distribution.

Following the MAP principle, the posteriori PDF of sparse noise $\mathbf{v}$ can be expressed as

$$p(\mathbf{v}|\mathbf{x}; \mathbf{b}) \propto p(\mathbf{x}|\mathbf{v}; \mathbf{b})p(\mathbf{v})$$
$$= C_1 \exp \left\{ -\frac{1}{\sigma_u^2} ||\mathbf{x} - (\mathbf{S}^T \otimes \mathbf{I}_M)\mathbf{b} - \mathbf{v}||_2^2 - \frac{C_2}{\sigma_v^\beta} ||\mathbf{v}||_\beta^\beta \right\} \tag{7}$$

where $C_1 = [\beta \Gamma(4/\beta)]^{MN} / [2\pi^2 \sigma_u^2 \sigma_v^2 \Gamma^2(2/\beta)]^{MN}$, and $C_2 = [\Gamma(4/\beta)/\Gamma(2/\beta)]^{\beta/2}$ are constants.

Applying negative logarithmic operation to (7) and ignoring constants and irrelevant items, $\mathbf{b}$ and $\mathbf{v}$ can be obtained by

$$\{\hat{\mathbf{b}}, \hat{\mathbf{v}}\} = \arg \ \min_{\mathbf{b},\mathbf{v}} ||\mathbf{x} - (\mathbf{S}^T \otimes \mathbf{I}_M)\mathbf{b} - \mathbf{v}||_2^2 + \mu ||\mathbf{v}||_\beta^\beta \qquad (8)$$

where μ is a tunable parameter. In reality, since the true approximated shape parameter β of sparse noise $\mathbf{v}$ cannot be easily obtained, we can replace β in (8) by a general parameter p with $0 < p < 2$, leading to the following result

$$\{\hat{\mathbf{b}}, \hat{\mathbf{v}}\} = \arg \ \min_{\mathbf{b},\mathbf{v}} ||\mathbf{x} - (\mathbf{S}^T \otimes \mathbf{I}_M)\mathbf{b} - \mathbf{v}||_2^2 + \mu ||\mathbf{v}||_p^p \qquad (9)$$

The above formulation is called a generalized ℓ_2-ℓ_p minimization, since the conventional ℓ_2-ℓ_p minimization problem contains only one unknown vector, while (9) has two unknown vectors $\mathbf{b}$ and $\mathbf{v}$.

3.2. Solution with dimension reduction

Based on extensive simulations similar to Example 1 in Section 4, to obtain a better performance, $0 < p < 1$ is required. When $0 < p < 1$, (9) becomes nonconvex and nonsmooth, where its global minimum cannot be easily guaranteed.

Many algorithms have been developed to solve the conventional ℓ_2-ℓ_p minimization problem, such as alternating direction method of multipliers (ADMM)[30, 31], and iteratively reweighted least squares (IRLS)[32–34]. Although ADMM can be applied directly to solve the problem in (9), it has a very slow convergence rate. An accelerated proximal gradient (APG) framework was proposed for nonconvex optimization with a fast convergence rate in [35]. To apply it here, we need to transform (9) into the conventional ℓ_2-ℓ_p

minimization problem. First, by fixing $\mathbf{v}$, (9) can be written as

$$\arg \min_{\mathbf{b}} ||\mathbf{x} - (\mathbf{S}^T \otimes \mathbf{I}_M)\mathbf{b} - \mathbf{v}||_2^2$$

$$= \arg \min_{\mathbf{B}} ||\mathbf{X} - \mathbf{B}\mathbf{S} - \mathbf{V}||_F^2$$

$$= \arg \min_{\mathbf{B}} ||(\mathbf{X}^T - \mathbf{V}^T) - \mathbf{S}^T\mathbf{B}^T||_F^2 \tag{10}$$

The least squares estimate of $\mathbf{B}^T$ can be obtained as

$$\hat{\mathbf{B}}^T = (\mathbf{S}^T)^\dagger(\mathbf{X}^T - \mathbf{V}^T) \tag{11}$$

Substituting (11) into (10), we have

$$||\mathbf{x} - (\mathbf{S}^T \otimes \mathbf{I}_M)\mathbf{b} - \mathbf{v}||_2^2$$

$$= ||(\mathbf{X}^T - \mathbf{V}^T) - \mathbf{S}^T(\mathbf{S}^T)^\dagger(\mathbf{X}^T - \mathbf{V}^T)||_F^2$$

$$= ||\mathbf{P}_{\mathbf{S}^T}^\perp \mathbf{V}^T - \mathbf{P}_{\mathbf{S}^T}^\perp \mathbf{X}^T||_F^2$$

$$= ||(\mathbf{I}_M \otimes \mathbf{P}_{\mathbf{S}^T}^\perp)\tilde{\mathbf{v}} - (\mathbf{I}_M \otimes \mathbf{P}_{\mathbf{S}^T}^\perp)\tilde{\mathbf{x}}||_2^2 \tag{12}$$

where $\mathbf{P}_{\mathbf{S}^T}^\perp = \mathbf{I}_N - \mathbf{S}^T(\mathbf{S}^T)^\dagger$, $\tilde{\mathbf{v}} = \text{vec}\{\mathbf{V}^T\}$, and $\tilde{\mathbf{x}} = \text{vec}\{\mathbf{X}^T\}$.

Utilizing (12), (9) can be expressed as

$$\hat{\mathbf{v}} = \arg \min_{\mathbf{v}} ||(\mathbf{I}_M \otimes \mathbf{P}_{\mathbf{S}^T}^\perp)\tilde{\mathbf{v}} - (\mathbf{I}_M \otimes \mathbf{P}_{\mathbf{S}^T}^\perp)\tilde{\mathbf{x}}||_2^2 + \mu||\tilde{\mathbf{v}}||_p^p \tag{13}$$

where the estimates of $\mathbf{b}$ and $\mathbf{v}$ are decoupled and the dimension of optimization is reduced. (13) is a standard ℓ_2-ℓ_p minimization problem and can be solved using the nonconvex APG framework [35]. However, the vectorization operator generates a very large matrix $(\mathbf{I}_M \otimes \mathbf{P}_{\mathbf{S}^T}^\perp)$ and long vectors $\tilde{\mathbf{x}}$ and $\tilde{\mathbf{v}}$.

To estimate the sparse noise part with lower computational complexity further, recalling that the ℓ_p norm of a vector is $||\mathbf{v}||_p^p = \sum_{i=1}^{MN} |v_i|^p$, (13) can be rewritten as

$$\hat{\mathbf{v}} = \arg \min_{\mathbf{v}} \sum_{m=1}^{M} ||\mathbf{P}_{\mathbf{S}^T}^\perp \tilde{\mathbf{v}}_m - \tilde{\mathbf{x}}_m||_2^2 + \mu||\tilde{\mathbf{v}}_m||_p^p \tag{14}$$

where $\tilde{\mathbf{v}}_m = \mathbf{V}_{m,:}^T$ and $\tilde{\mathbf{x}}_m = \mathbf{P}_{\mathbf{S}^T}^{\perp}\mathbf{X}_{m,:}^T$ with $\mathbf{V}_{m,:}$ and $\mathbf{X}_{m,:}$ denoting the mth row of $\mathbf{V}$ and $\mathbf{X}$, respectively. Since $||\mathbf{P}_{\mathbf{S}^T}^{\perp}\tilde{\mathbf{v}}_m - \tilde{\mathbf{x}}_m||_2^2 + \mu||\tilde{\mathbf{v}}_m||_p^p$ is nonnegative, the optimization problem can be solved in parallel with M independent small scale ℓ_2-ℓ_p minimizations.

Table 1: Solution to (14) via APG.

Input:$\{\tilde{\mathbf{x}}_m\}_{m=1}^M$, $\mathbf{P}_{\mathbf{S}^T}^{\perp}$, $\{\tilde{\mathbf{v}}_m^{(0)}\}_{m=1}^M$, p, μ, κ, maxIter, ε, $\rho^{(0)}$

Ouput:$\{\tilde{\mathbf{v}}_m\}_{m=1}^M$

1: FOR $m = 1$ to M

2:     Set $t = 0$, $\rho^{(-1)} = \rho^{(0)}$, $\mathbf{z}_m^{(-1)} = \tilde{\mathbf{v}}_m^{(0)}$, $\tilde{\mathbf{v}}_m^{(1)} = \tilde{\mathbf{v}}_m^{(0)}$;

3:     WHILE ($t \leq$ maxIter)

4:        $\mathbf{y}_m^{(t)} = \tilde{\mathbf{v}}_m^{(t)} + \frac{\rho^{(t-1)}}{\rho^{(t)}}(\mathbf{z}_m^{(t)} - \tilde{\mathbf{v}}_m^{(t)}) + \frac{\rho^{(t-1)}-1}{\rho^{(t)}}(\tilde{\mathbf{v}}_m^{(t)} - \tilde{\mathbf{v}}_m^{(t-1)})$;

5:        $\mathbf{z}_m^{(t+1)} = \text{prox}_{h,\kappa}(\mathbf{y}_m^{(t)} - \frac{1}{2\kappa}(\mathbf{P}_{\mathbf{S}^T}^{\perp})^H(\mathbf{P}_{\mathbf{S}^T}^{\perp}\mathbf{y}_m^{(t)} - \tilde{\mathbf{x}}_m))$;

6:        $\mathbf{r}_m^{(t+1)} = \text{prox}_{h,\kappa}(\tilde{\mathbf{v}}_m^{(t)} - \frac{1}{2\kappa}(\mathbf{P}_{\mathbf{S}^T}^{\perp})^H(\mathbf{P}_{\mathbf{S}^T}^{\perp}\tilde{\mathbf{v}}_m^{(t)} - \tilde{\mathbf{x}}_m))$;

7:        $F(\mathbf{z}_m^{(t+1)}) = ||\mathbf{P}_{\mathbf{S}^T}^{\perp}\mathbf{z}_m^{(t+1)} - \tilde{\mathbf{x}}_m||_2^2 + \mu||\mathbf{z}_m^{(t+1)}||_p^p$;

          $F(\mathbf{r}_m^{(t+1)}) = ||\mathbf{P}_{\mathbf{S}^T}^{\perp}\mathbf{r}_m^{(t+1)} - \tilde{\mathbf{x}}_m||_2^2 + \mu||\mathbf{r}_m^{(t+1)}||_p^p$;

8:        IF $(F(\mathbf{z}_m^{(t+1)}) \leq F(\mathbf{r}_m^{(t+1)}))$ $\tilde{\mathbf{v}}_m^{(t+1)} = \mathbf{z}_m^{(t+1)}$;   ELSE $\tilde{\mathbf{v}}_m^{(t+1)} = \mathbf{r}_m^{(t+1)}$;

9:        IF $(\frac{||\tilde{\mathbf{v}}_m^{(t+1)} - \tilde{\mathbf{v}}_m^{(t)}||_2^2}{\sqrt{||\tilde{\mathbf{v}}_m^{(t+1)}||_2 \cdot ||\tilde{\mathbf{v}}_m^{(t)}||_2}} \leq \varepsilon)$ BREAK;

10:       $\rho^{(t+1)} = \frac{\sqrt{4(\rho^{(t)})^2 + 1} + 1}{2}$;

11:       $t = t + 1$;

Now the nonconvex acceleration framework in [35] is utilized M times to solve (14), and the corresponding algorithm is listed in Table 1. κ is the Lipschitz constant of the gradient of $||\mathbf{P}_{\mathbf{S}^T}^{\perp}\tilde{\mathbf{v}}_m - \tilde{\mathbf{x}}_m||_2^2$ with respect to $\tilde{\mathbf{v}}_m$, and can be obtained by the maximum eigenvalue of $(\mathbf{P}_{\mathbf{S}^T}^{\perp})^H\mathbf{P}_{\mathbf{S}^T}^{\perp}$. In Lines

5-6, "prox" denotes the proximal operator of a function, defined as

$$\text{prox}_{h,\kappa}(\mathbf{f}) = \arg \min_{\tilde{\mathbf{v}}_m} h(\tilde{\mathbf{v}}_m) + \frac{\kappa}{2} ||\mathbf{f} - \tilde{\mathbf{v}}_m||_2^2 \tag{15}$$

where $h(\tilde{\mathbf{v}}_m) = \mu||\tilde{\mathbf{v}}_m||_p^p$. With the proximal mapping, $\text{prox}_{h,\kappa}(\mathbf{f})$ reduces to solving N univariate minimization problems. Moreover, for $0 < p < 1$, the solution to (15) can be expressed as follows [29, 36]:

$$\text{prox}_{h,\kappa}(\mathbf{f})_n = \begin{cases} 0 & |f_n| \leq \tau \\ \text{sign}(f_n)\xi_n & |f_n| > \tau \end{cases} \tag{16}$$

where $n = 0, 1, \cdots, N-1$, $\text{sign}(\cdot)$ is the sign function with $\text{sign}(c) = c/|c|$ for a complex number c, and $|\cdot|$ represents the modulus of a complex number. $\tau = \vartheta + \mu p \vartheta^{p-1}/\kappa$, and $\vartheta = [2\mu(1-p)/\kappa]^{1/(2-p)}$. ξ_n can be obtained from the root of $\tilde{h}_n(\xi) = \mu p \xi^{p-1} + \kappa\xi - \kappa|f_n|$ within the range $(\vartheta, |f_n|)$, which can be solved via the Newton algorithm since $\tilde{h}_n(\xi)$ is convex [37].

The algorithm requires initializations $\{\tilde{\mathbf{v}}_m^{(0)}\}_{m=1}^M$ in Table 1, and we can obtain reliable initial values via setting $p = 1$ firstly, i.e., solving the convex ℓ_2-ℓ_1 optimization. For $p = 1$, there is a closed-form solution to (15)

$$\text{prox}_{h,\kappa}(\mathbf{f})_n = \text{sign}(f_n) \max\{|f_n| - \mu/\kappa\} \tag{17}$$

Moreover, with the estimate $\{\hat{\mathbf{v}}_m\}_{m=1}^M$ of sparse noise part via the method in Table 1, we can obtain the data model in Gaussian noise,

$$\tilde{\mathbf{X}} = \mathbf{X} - \hat{\mathbf{V}} \approx \mathbf{B}\mathbf{S} + \mathbf{U} \tag{18}$$

where $\hat{\mathbf{V}} = [\hat{\mathbf{v}}_1, \hat{\mathbf{v}}_2, \cdots, \hat{\mathbf{v}}_M]^T$.

Then, we can obtain the estimate of $\mathbf{B}$ via the least squares method

$$\hat{\mathbf{B}} = \tilde{\mathbf{X}}\mathbf{S}^\dagger \tag{19}$$

10

Utilizing the structural information of $\hat{\mathbf{B}}$ and inspired by [16], DOA and complex amplitude can be estimated as follows

$$\hat{\theta}_q = \arg \ \min_{\theta} |\hat{\mathbf{b}}_q^H \mathbf{P}_{\mathbf{a}(\theta)}^{\perp} \hat{\mathbf{b}}_q| \tag{20}$$

$$\hat{g}_q = \frac{1}{M} \sum_{m=1}^{M} \frac{\hat{\mathbf{B}}_{m,q}}{\exp\{-j2\pi(m-1)d\sin\hat{\theta}_q/\lambda\}} \tag{21}$$

where $\hat{\mathbf{b}}_q$ and $\hat{\mathbf{B}}_{m,q}$ represent the qth column and (m,q)th element of $\hat{\mathbf{B}}$, respectively. $\mathbf{P}_{\mathbf{a}(\theta)}^{\perp} = \mathbf{I}_M - \mathbf{a}(\theta)\mathbf{a}^{\dagger}(\theta)$.

3.3. Summary of the proposed method

Steps of the proposed method is summarized as follows:

Step 1: Setting $p = 1$, obtain the initial estimation of $\{\tilde{\mathbf{v}}_m^{(0)}\}_{m=1}^{M}$ by the proposed approach in Table 1, where the initial values $\{\tilde{\mathbf{v}}_m^{(0)}\}_{m=1}^{M}$ for $p = 1$ can be a zero vector.

Step 2: Following the method in in Table 1, with $\{\tilde{\mathbf{v}}_m^{(0)}\}_{m=1}^{M}$ and $0 < p < 1$, obtain the final estimate $\{\hat{\mathbf{v}}_m\}_{m=1}^{M}$.

Step 3: Utilize (19) to obtain $\hat{\mathbf{B}}$, and calculate the estimates of DOAs and complex amplitudes from (20)-(21).

Remark 1: Similar to DEML [7] and WCDEML [13], for common scenarios, the proposed method can hold for $Q < N, M < N$, while Q can be smaller than, equal to or larger than M.

Remark 2: The tuning parameters p and μ are obtained in an empirical way via simulations in Section 4.

4. Simulation Results

In this section, numerical simulations are conducted to demonstrate the performance of the proposed method compared with those of EM [19], ℓ_p [20], SC [23], IMLE [24], ln-ℓ_p^ε[26], and the CRB for known waveforms in impulsive noise (see the supplementary material for detailed derivation). [2]

Since the proposed method has split the noise into Gaussian and sparse components, we called it NGSC (Noise Gaussianization with Sparse Constraint) for short. The common parameters are $M = 4$, and $d = \lambda/2$, and the known waveforms of all sources are of unit power. For NGSC, simulations are performed to determine the best values for p and μ (see the following Example 1 for details), where maxIter $= 1000$, $\varepsilon = 10^{-6}$, and $\rho^{(0)} = 10^3$. Three types of impulsive noise, namely, GMM, GGD, and SαS distributions, are utilized for simulations. [3]

1) GMM: The PDF of the two-term complex circular Gaussian mixture

---

[2]The original ℓ_p [20] and SC [23] cannot be applied directly to DOA estimation for sources with known waveforms. Here, we only use them to estimate $\mathbf{B}$ with known $\mathbf{S}$, and the DOAs and complex amplitudes are obtained from (20)-(21). For EM [19], the estimation of waveform in (22) of [19] is replaced by complex amplitude estimation, i.e., $\mathbf{g} = (\mathbf{S}^T \odot \mathbf{A})^{-1}\text{vec}\{\mathbf{X}\}$, where $\odot$ denotes the Khatri-Rao product. In terms of IMLE [24], the signal waveform $\mathbf{s}(t)$ in (1) of [24] is known.

[3]It can be shown that SIRP and CES noises could also be decomposed into Gaussian plus sparse outliers in (2) with some acceptable approximation errors. Therefore, the effectiveness of the proposed method can also be examined for these two noise models. For consistency with the compared methods, ℓ_p, SC and ln-ℓ_p^ε, here they are not considered.

noise $w(n)$ is given by

$$p_w(w) = \sum_{i=1}^{2} \frac{c_i}{\pi \sigma_i^2} \exp\left(-\frac{|w|^2}{\sigma_i^2}\right) \tag{22}$$

where $0 < c_i \leq 1$ and σ_i^2 are the probability and variance of the ith term, respectively, with $c_1 + c_2 = 1$. If $\sigma_2^2 \gg \sigma_1^2$ and $c_2 < c_1$ are chosen, samples of larger variance σ_2^2 occurring with smaller probability c_2 are treated as outliers in the presence of Gaussian background noise of smaller variance σ_1^2 with larger probability c_1. In the following simulations, $\sigma_2^2 = 10^3 \sigma_1^2$, $c_2 = 0.2$, and $\sigma_w^2 = c_1\sigma_1^2 + c_2\sigma_2^2 = 0.1$. The corresponding signal to noise ratio (SNR) is defined as $\text{SNR} = \sigma_s^2/\sigma_w^2$ with σ_s^2 being the power of source signal.

2) GGD: Following (6), the PDF of circular zero-mean GGD with variance σ_w^2 is given by

$$p_w(w) = \frac{\beta\Gamma(4/\beta)}{2\pi\sigma_w^2\Gamma^2(2/\beta)} \exp\left\{-\left[\frac{\Gamma(4/\beta)}{\Gamma(2/\beta)}\right]^{\frac{\beta}{2}} \frac{|w|^\beta}{\sigma_w^\beta}\right\} \tag{23}$$

where the parameters are set to $\beta = 0.3$ and $\sigma_w^2 = 0.1$. Its SNR has the same definition as that of GMM noise.

3) SαS: Since there is no closed-form expression for the PDF of SαS distribution except for $\alpha = 1$ and $\alpha = 2$, it is often represented by its characteristic function $\varphi(\omega) = \exp(-\gamma^\alpha|\omega|^\alpha)$, where $\alpha \in (0, 2]$ is called the characteristic exponent, and $\gamma > 0$ denotes the scale parameter. When $\alpha = 1$, SαS distribution reduces to the Cauchy one, while $\alpha = 2$, to Gaussian. Because the second-order and higher-order moments of the SαS distribution are infinite for $\alpha < 2$, the generalized SNR (GSNR) is used instead, i.e., $\text{GSNR} = \sigma_s^2/\gamma^\alpha$. In our simulations, $\alpha = 1.0$ and $\gamma = 0.1$.

Example 1: The optimal tuning parameters p and μ are determined in the presence of GMM noises. The DOAs and complex amplitudes of two

13
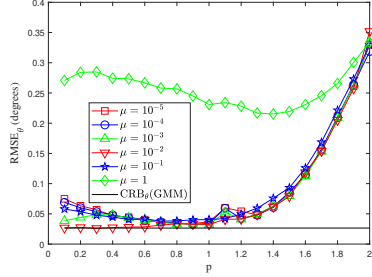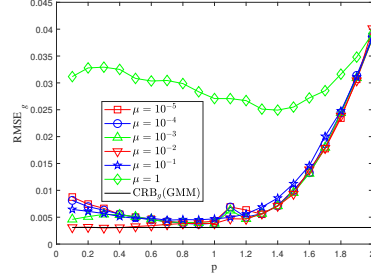
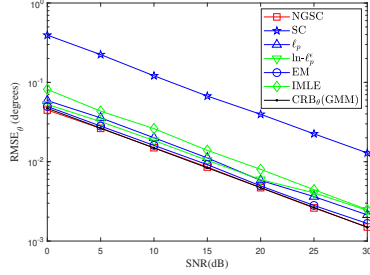(a) DOA   (b) Complex amplitude

Figure 1: RMSE versus p and μ for GMM noises, with $Q = 2$, $M = 4$, SNR $= 5$ dB, and $N = 100$.

sources are set to $10°$, $15°$, $e^{j0.3\pi}$, and $e^{-j0.4\pi}$, respectively. With SNR $= 5$ dB and $N = 100$, the root mean square error (RMSE) results based on 500 Monte Carlo trials for each fixed p and μ are shown in Fig. 1. It can be seen that the estimation performance can be improved with suitable p and μ, especially for $0 < p < 1$. Moreover, the best parameters under current settings are $p = 0.3$, and $\mu = 0.01$, which are chosen for Examples 2 & 3.

Similarly, the best parameters for ℓ_p and ln-ℓ_p^ε are determined $p = 1.1$, and $\varepsilon = 0.01$ for GMM, GGD, and SαS noises. For parameter determination, ℓ_p and ln-ℓ_p^ε have shown more robustness than NGSC.

Example 2: The performance with respect to SNR in the presence of GMM noises is investigated. The settings are the same as those in Example 1 except that SNR varies from 0 dB to 30 dB with an interval of 5 dB. Fig. 2 shows the results.
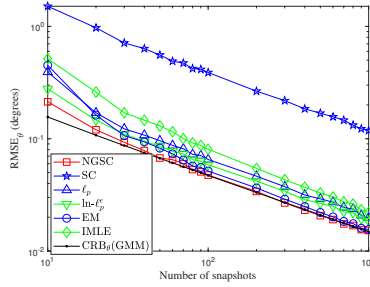
Examples 3: The performance against the number of snapshots is examined. The settings are the same as those in Example 1 except that SNR $= 5$ dB, and N varies from 10 to 1000. The results are provided in Fig. 3.
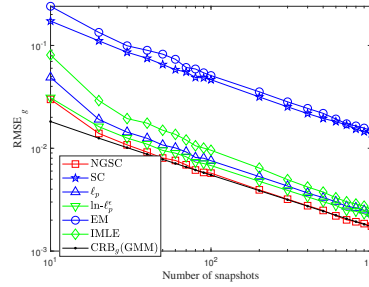
14
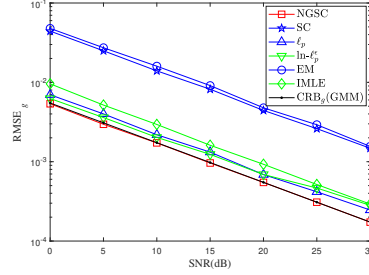
(a) DOA

(b) Complex amplitude

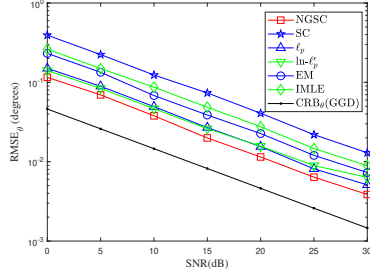Figure 2: RMSE versus SNR for GMM noises, with $Q = 2$, $M = 4$, and $N = 100$.
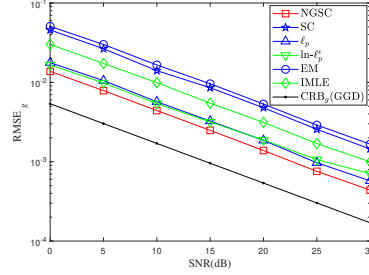

(a) DOA

(b) Complex amplitude

Figure 3: RMSE versus the number of snapshots, with $Q = 2$, $M = 4$, and SNR = 5 dB.

As shown in Figs. 2 and 3, NGSC can work for ranges of SNR from 0dB to 30dB and N from 10 to 1000 effectively. Moreover, it outperforms the other four methods, has similar angle estimation performance to EM under GMM noises, and can approach CRB for high SNR values and with a large number of snapshots in the presence of GMM noises.
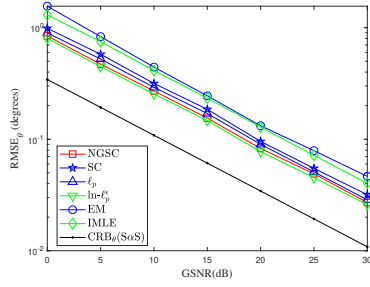
Examples 4: Now consider GGD noises. $p = 0.8$ and $\mu = 0.01$ are determined via simulations similar to Example 1. The other settings are the same as those in Example 2. Fig. 4 shows the results. Similar to Fig. 2, NGSC can also be effective in GGD noise and has achieved better angle and
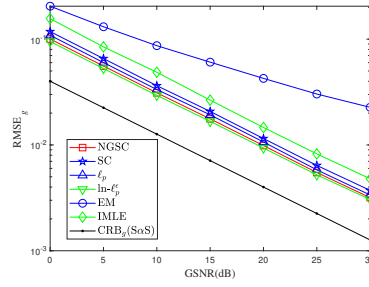
15

(a) DOA   (b) Complex amplitude

Figure 4: RMSE versus SNR for GGD noises, with $Q = 2$, $M = 4$, and $N = 100$.

(a) DOA   (b) Complex amplitude

Figure 5: RMSE versus GSNR for SαS noises, with $Q = 2$, $M = 4$, and $N = 100$.

complex amplitude estimations than the other five methods. However, since there is a relatively large difference between the mechanisms of GMM and GGD, NGSC can not provide a very close performance to CRB for GGD noise.

Examples 5: the performance of the proposed method with respect to GSNR under SαS noises is studied. Its optimal parameters are $p = 0.8$ and $\mu = 0.01$. The other settings are the same as those in Example 1. The estimation results are presented in Fig. 5, where the proposed NGSC method shows a similar performance to ℓ_p and ln-ℓ_p^ε, and better than SC, EM, and IMLE.

16

Compared with Example 1, possible reason for the performance degradation may be the same as in Example 3, i.e., the relatively large difference between the mechanisms of GMM and SαS.

5. Conclusions

A novel DOA estimation method for sources called NGSC with known waveforms in the presence of impulsive noise has been introduced. Based on the MAP principle and by dividing the impulsive noise into Gaussian and sparse parts, a generalized ℓ_2-ℓ_p minimization cost function was constructed. With orthogonal projection and the component additivity of ℓ_p norm, multiple independent and dimension reduced simple ℓ_2-ℓ_p optimization problems were formulated and solved through the APG framework; finally, the DOAs and complex amplitudes were obtained based on the cleaned data via removing the sparse noise part. As demonstrated by computer simulations, NGSC has outperformed existing algorithms for GMM and GGD noise, and with a comparable performance for SαS noise; it can achieve the CRB for cases with a high SNR and a large number of snapshots in the presence of GMM noise. In addition, the proposed solution is general and can be applied to other impulsive or heavy-tailed noise models, such as CES and SIRP.

References

[1] H. L. Van Trees, Detection, estimation, and modulation theory, optimum array processing, John Wiley & Sons, 2004.

[2] P. Stoica, K. Sharman, Maximum likelihood methods for direction-of-arrival estimation, IEEE Trans. Acoust., Speech, Signal Process. 38 (7) (1990) 1132–1143.

[3] M. Viberg, B. Ottersten, Sensor array processing based on subspace fining, IEEE Trans. Signal Process. 39 (5) (1991) 1110–1121.

[4] R. O. Schmidt, Multiple emitter location and signal parameter estimation, IEEE Trans. Antennas Propag. 34 (3) (1986) 276–280.

[5] R. Roy, T. Kailath, ESPRIT-estimation of signal parameters via rotational invariance techniques, IEEE Trans. Acoust., Speech, Signal Process., 37 (7) (1989) 984–995.

[6] J. Li, R. Compton, Maximum likelihood angle estimation for signals with known waveforms, IEEE Trans. Signal Process. 41 (9) (1993) 2850–2862.

[7] J. Li, B. Halder, P. Stoica, M. Viberg, Computationally efficient angle estimation for signals with known waveforms, IEEE Trans. Signal Process. 43 (9) (1995) 2154–2163.

[8] N. Wang, P. Agathoklis, A. Antoniou, A new DOA estimation technique based on subarray beamforming, IEEE Trans. Signal Process. 54 (9) (2006) 3279–3290.

[9] J.-F. Gu, W.-P. Zhu, M. Swamy, Fast and efficient DOA estimation method for signals with known waveforms using nonuniform linear arrays, Signal Process. 114 (2015) 265–276.

[10] J.-F. Gu, W.-P. Zhu, M. Swamy, Direction of arrival tracking for signals with known waveforms based on block least squares techniques, J. Frankl. Inst. 354 (11) (2017) 4573–4594.

[11] Y.-Y. Dong, C.-X. Dong, W. Liu, M.-M. Liu, Z. Tang, A structure-aware DOA estimation method for sources with short known waveforms, IEEE Access 6 (2018) 71271–71278.

[12] M. Cedervall, R. L. Moses, Efficient maximum likelihood DOA estimation for signals with known waveforms in the presence of multipath, IEEE Trans. Signal Process. 45 (3) (1997) 808–811.

[13] H. Li, G. Liu, J. Li, Angle estimator for signals with known waveforms, Electron. Lett. 35 (23) (1999) 1992–1994.

[14] L. N. Atallah, S. Marcos, DOA estimation and association of coherent multipaths by using reference signals, Signal Process. 84 (6) (2004) 981–996.

[15] J.-F. Gu, P. Wei, H.-M. Tai, Fast direction-of-arrival estimation with known waveforms and linear operators, IET Signal Process. 2 (1) (2008) 27–36.

[16] A. L. Swindlehurst, Time delay and spatial signature estimation using known asynchronous signals, IEEE Trans. Signal Process. 46 (2) (1998) 449–462.

[17] Y.-Y. Dong, C.-X. Dong, W. Liu, M.-M. Liu, Z.-Z. Tang, Robust DOA estimation for sources with known waveforms against Doppler shifts via oblique projection, IEEE Sens. J. 18 (16) (2018) 6735–6742.

[18] Y.-Y. Dong, C.-X. Dong, W. Liu, M.-M. Liu, DOA estimation with known waveforms in the presence of unknown time delays and Doppler shifts, Signal Process. 166 (2020) 107232.

[19] R. J. Kozick, B. M. Sadler, Maximum-likelihood array processing in non-Gaussian noise with Gaussian mixtures, IEEE Trans. Signal Process. 48 (12) (2000) 3520–3535.

[20] W. Zeng, H. C. So, L. Huang, ℓ_p-MUSIC: Robust direction-of-arrival estimator for impulsive noise environments, IEEE Trans. Signal Process. 61 (17) (2013) 4296–4308.

[21] P. Tsakalides, C. L. Nikias, The robust covariation-based MUSIC (ROC-MUSIC) algorithm for bearing estimation in impulsive noise environments, IEEE Trans. Signal Process. 44 (7) (1996) 1623–1633.

[22] T.-H. Liu, J. M. Mendel, A subspace-based direction finding algorithm using fractional lower order statistics, IEEE Trans. Signal Process. 49 (8) (2001) 1605–1613.

[23] J. F. Zhang, T.-s. Qiu, P. Wang, S.-y. Luan, A novel cauchy score function based DOA estimation method under alpha-stable noise environments, Signal Process. 138 (2017) 98–105.

[24] X. Zhang, M. N. E. Korso, M. Pesavento, MIMO radar target localization and performance evaluation under SIRP clutter, Signal Process. 130 (2017) (2017) 217–232.

[25] E. Ollila, D. E. Tyler, V. Koivunen, H. V. Poor, Complex elliptically symmetric distributions: Survey, new results and applications, IEEE Trans. Signal Process. 60 (11) (2012) 5597–5625.

[26] Y.-Y. Dong, C.-X. Dong, Z.-G. Wu, J. Cai, H. Chen, Robust DOA estimation for sources with known waveforms in impulsive noise environments, in: 2020 IEEE 11th Sensor Array Multichannel Signal Process. Workshop (SAM), 2020, pp. 1–5.

[27] J. Dai, H. C. So, Sparse Bayesian learning approach for outlier-resistant direction-of-arrival estimation, IEEE Trans. Signal Process. 66 (3) (2018) 744–756.

[28] R. Zheng, X. Xu, Z. Ye, J. Dai, Robust sparse bayesian learning for DOA estimation in impulsive noise environments, Signal Process. 171 (2020) 107500.

[29] F. Wen, P. Liu, Y. Liu, R. C. Qiu, W. Yu, Robust sparse recovery in impulsive noise via ℓ_p-ℓ_1 optimization, IEEE Trans. Signal Process. 65 (1) (2017) 105–118.

[30] S. Boyd, N. Parikh, E. Chu, B. Peleato, J. Eckstein, Distributed optimization and statistical learning via the alternating direction method of multipliers, Found. Trends Mach. Learn. 3 (1) (2010) 1–122.

[31] Y. Wang, W. Yin, J. Zeng, Global convergence of ADMM in nonconvex nonsmooth optimization, J. Sci. Comput. 78 (2019) 29–63.

[32] S. Foucart, M. J. Lai, Sparsest solutions of underdetermined linear systems via ℓ_q-minimization for $0 < q \leq 1$, Applied Computational Harmon. Anal. 26 (3) (2009) 395–407.

[33] I. Daubechies, R. Devore, M. Fornasier, C. S. Gunturk, Iteratively reweighted least squares minimization for sparse recovery, Commun. Pure Appl. Math. 63 (1) (2010) 1–38.

[34] M.-J. Lai, Y. Xu, W. Yin, Improved iteratively reweighted least squares for unconstrained smoothed ℓ_q minimization, SIAM J. Numer. Anal. 51 (2) (2013) 927–957.

[35] H. Li, Z. Lin, Accelerated proximal gradient methods for nonconvex programming, in: Adv. Neural Inf. Process. Syst. 28 (NIPS 2015), 2015, pp. 379–387.

[36] G. Marjanovic, V. Solo, On ℓ_q optimization and matrix completion, IEEE Trans. Signal Process. 60 (11) (2012) 5714–5724.

[37] S. Boyd, L. Vandenberghe, Convex Optimization, Cambridge University Press, 2004.

Generalized ℓ_2-ℓ_p Minimization Based DOA Estimation for Sources with Known Waveforms in Impulsive Noise ——Supplementary Material

Yang-Yang Dong[a,*], Chun-Xi Dong[a], Wei Liu[b], Jingjing Cai[a]

[a]*School of Electronic Engineering, Xidian University, Xi'an 710071, China*
[b]*Department of Electronic and Electrical Engineering, University of Sheffield, S1 4ET, U.K.*

Appendix : Derivation of the CRB

Similar to [1, 2], we firstly construct a vector consisting of all real-valued unknown variables of the data model in (1) of the corresponding paper

$$\boldsymbol{\mu} = [\boldsymbol{\theta}^T, \boldsymbol{\xi}^T, \boldsymbol{\eta}^T]^T \tag{1}$$

where $\boldsymbol{\xi} = [\xi_1, \cdots, \xi_Q]^T = [\mathrm{Re}(g_1), \cdots, \mathrm{Re}(g_Q)]^T$, $\boldsymbol{\eta} = [\xi_1, \cdots, \xi_Q]^T = [\mathrm{Im}(g_1), \cdots, \mathrm{Im}(g_Q)]^T$.

For simplicity, $\mathbf{A}(\boldsymbol{\theta})$ and $\mathbf{G}(\mathbf{g})$ are denoted as $\mathbf{A}$ and $\mathbf{G}$, and we have $\mathbf{x}_0(n) = \mathbf{AGs}(n)$.

Similar to [1, 2], the corresponding Fisher information matrix can be derived as follows,

$$\mathbf{I}(\boldsymbol{\mu}) = \frac{1}{I_c} \mathrm{Re} \left\{ \begin{bmatrix} \mathbf{I}_{\theta\theta} & \mathbf{I}_{\theta\xi} & \mathbf{I}_{\theta\eta} \\ \mathbf{I}_{\xi\theta} & \mathbf{I}_{\xi\xi} & \mathbf{I}_{\xi\eta} \\ \mathbf{I}_{\eta\theta} & \mathbf{I}_{\eta\xi} & \mathbf{I}_{\eta\eta} \end{bmatrix} \right\} \tag{2}$$

*Corresponding author
Email address: dongyangyang2104@126.com (Yang-Yang Dong)

where

$$\mathbf{I}_{\boldsymbol{\theta\theta}} \quad = N \cdot (\mathbf{G^H} \dot{\mathbf{A}}^H \dot{\mathbf{A}} \mathbf{G}) \circ \mathbf{R}_{ss}^T \tag{3}$$

$$\mathbf{I}_{\boldsymbol{\theta\xi}} = \mathbf{I}_{\boldsymbol{\xi\theta}}^H \quad = N \cdot (\mathbf{G}^H \dot{\mathbf{A}}^H \mathbf{A} \dot{\mathbf{G}}_\xi) \circ \mathbf{R}_{ss}^T \tag{4}$$

$$\mathbf{I}_{\boldsymbol{\theta\eta}} = \mathbf{I}_{\boldsymbol{\eta\theta}}^H \quad = N \cdot (\mathbf{G}^H \dot{\mathbf{A}}^H \mathbf{A} \dot{\mathbf{G}}_\eta) \circ \mathbf{R}_{ss}^T \tag{5}$$

$$\mathbf{I}_{\boldsymbol{\xi\xi}} \quad = N \cdot (\dot{\mathbf{G}}_\xi^H \mathbf{A}^H \mathbf{A} \dot{\mathbf{G}}_\xi) \circ \mathbf{R}_{ss}^T \tag{6}$$

$$\mathbf{I}_{\boldsymbol{\xi\eta}} = \mathbf{I}_{\boldsymbol{\eta\xi}}^H \quad = N \cdot (\dot{\mathbf{G}}_\xi^H \mathbf{A}^H \mathbf{A} \dot{\mathbf{G}}_\eta) \circ \mathbf{R}_{ss}^T \tag{7}$$

$$\mathbf{I}_{\boldsymbol{\eta\eta}} \quad = N \cdot (\dot{\mathbf{G}}_\eta^H \mathbf{A}^H \mathbf{A} \dot{\mathbf{G}}_\eta) \circ \mathbf{R}_{ss}^T \tag{8}$$

where $\dot{\mathbf{A}} = [\frac{\partial \mathbf{a}(\theta_1)}{\partial \theta_1}, \cdots, \frac{\partial \mathbf{a}(\theta_Q)}{\partial \theta_Q}]$, $\dot{\mathbf{G}}_\xi = [\frac{\partial \mathbf{G}_1}{\partial \xi_1}, \cdots, \frac{\partial \mathbf{G}_Q}{\partial \xi_q}]$, $\dot{\mathbf{G}}_\eta = [\frac{\partial \mathbf{G}_1}{\partial \eta_1}, \cdots, \frac{\partial \mathbf{G}_Q}{\partial \eta_q}]$, $\mathbf{R}_{ss} = 1/N \cdot \sum_{n=0}^{N-1} \mathbf{s}(n)\mathbf{s}^H(n)$. Besides,

$$I_c = \pi \int_0^\infty \frac{(p'_w(\rho))^2}{p_w(\rho)} \rho d\rho \tag{9}$$

where $\rho = |w|$ denotes the modulus of the complex variable w, and $p'_w(\rho)$ represents the first-order derivative of $p_w(\rho)$.

Therefore, with the relationship between CRB and the Fisher information matrix, we have

$$\mathrm{CRB}_\theta = \sqrt{1/Q \sum_{q=1}^Q \boldsymbol{\Delta}_{q,q}} \tag{10}$$

$$\mathrm{CRB}_g = \sqrt{1/Q \sum_{q=1}^Q (\boldsymbol{\Delta}_{Q+q,Q+q} + \boldsymbol{\Delta}_{2Q+q,2Q+q})} \tag{11}$$

where CRB_θ and CRB_g represent the Cramer-Rao bounds for DOAs and complex amplitudes, respectively. $\boldsymbol{\Delta} = \mathbf{I}^{-1}(\boldsymbol{\mu})$, and $\boldsymbol{\Delta}_{p,q}$ denotes the (p,q)th element of $\boldsymbol{\Delta}$.

References

[1] Y.-Y. Dong, C.-X. Dong, W. Liu, M.-M. Liu, Z.-Z. Tang, Robust DOA estimation for sources with known waveforms against Doppler shifts via oblique projection, IEEE Sens. J. 18 (16) (2018) 6735–6742.

[2] W. Zeng, H. C. So, L. Huang, ℓ_p-MUSIC: Robust direction-of-arrival estimator for impulsive noise environments, IEEE Trans. Signal Process. 61 (17) (2013) 4296–4308.